Antibacterial PMMA composite cements with tunable thermal and mechanical properties.

Arianna De Mori[a], Emanuela Di Gregorio[a], Alexander Peter Kao[b], Gianluca Tozzi[b], Eugen Barbu[a], Anita Sanghani-Kerai[c†], Roger R. Draheim[a] and Marta Roldo[a].*

[a] School of Pharmacy and Biomedical Science, University of Portsmouth, St Michael's Building, White Swan Road, PO1 2DT, Portsmouth, UK.

[b]Zeiss Global Centre, School of Mechanical and Design Engineering, University of Portsmouth, Anglesea Building, Anglesea Road, PO1 3DJ Portsmouth, UK.

[c]Institute of Orthopaedics and Muscoloskeletal Science, University College of London, Brockley Hill, Stanmore, HA7 4LP, London, UK.

KEYWORDS

Poly(methylmethacylate), chitosan, silver nanowires, bone cement

Figure S1. Light microscope images of **(A)** PMMA, **(B)** CS and **(C)** CSMCC particles. Magnification 10X. Scale bar 84.46 µm.

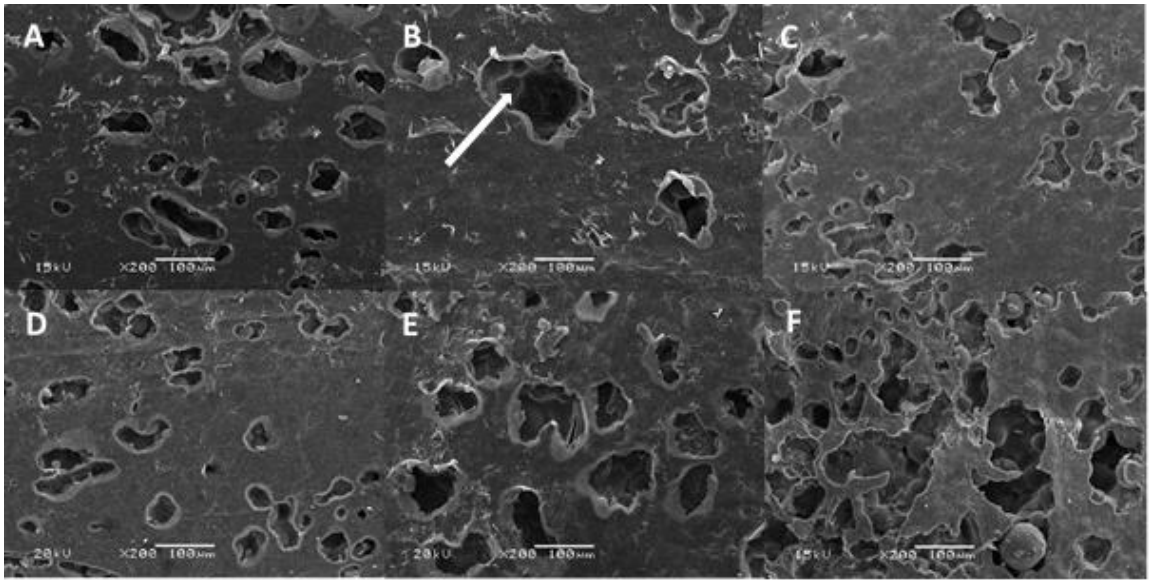

Figure S2. SEM images of cements surfaces. X200 magnification. **(A) and (D)** PMMA_2:0.8, **(B)** and **(E)** PMMA_2:0.8_CS20 and **(C) and (F)** PMMA_2:0.8_CSMCC20. Arrow indicates PMMA beads within the cement. SEM images of cement surfaces were taken before (A, B and C) and after (D, E and F) degradation in PBS for 4 weeks. Scale bar 100 µm.

The SEM images (Fig S2) revealed the presence of PMMA beads (arrow), incorporated into a homogeneously polymerized MMA cement interspersed with uneven holes of different diameters. These features can be attributed to the manual powder mixing method. Some previous studies have shown better osteoconductivity for substitutes with pore size between 200 and 600 µm, whereas other reports have shown no significant difference in osteoconductivity among different pore sizes.[1,2] Images showed an increased porosity on the cements surfaces before and after degradation, whenever CS/CSMCC were present in the formulation.

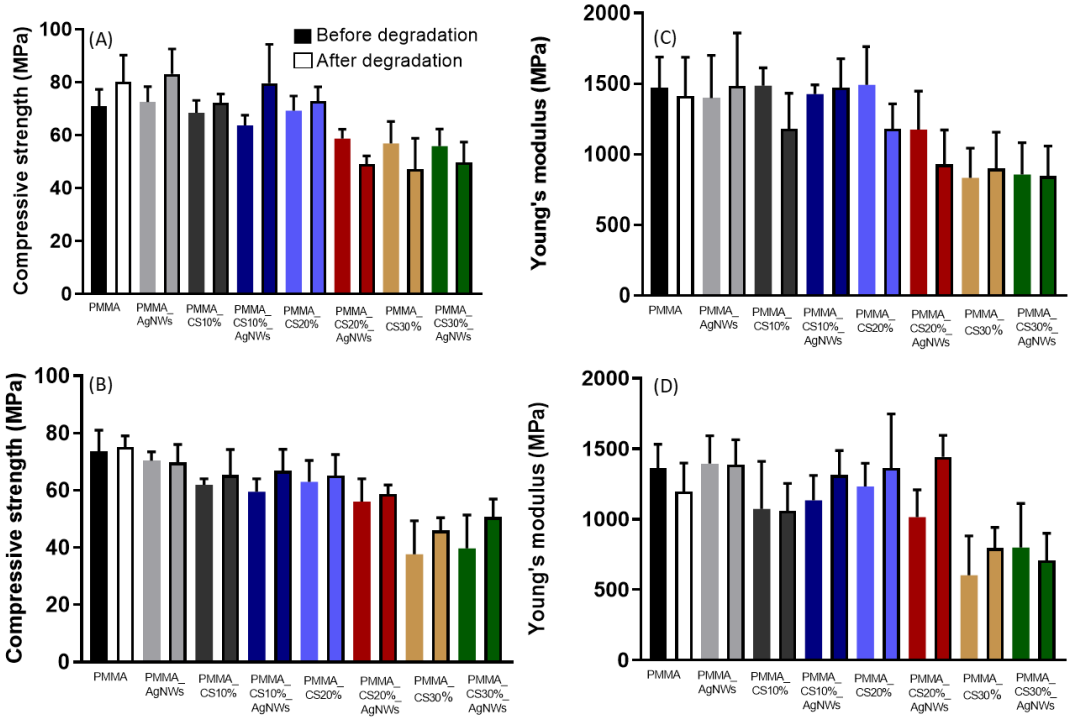

Figure S3. Compressive strength (**A** and **B**) and Young's modulus (**C** and **D**) of PMMA-based cements containing CS, before (no border) and after compression (black border). (A and C) cements with P/L 2:1 and (B and D) cements with P/L 2:0.8.

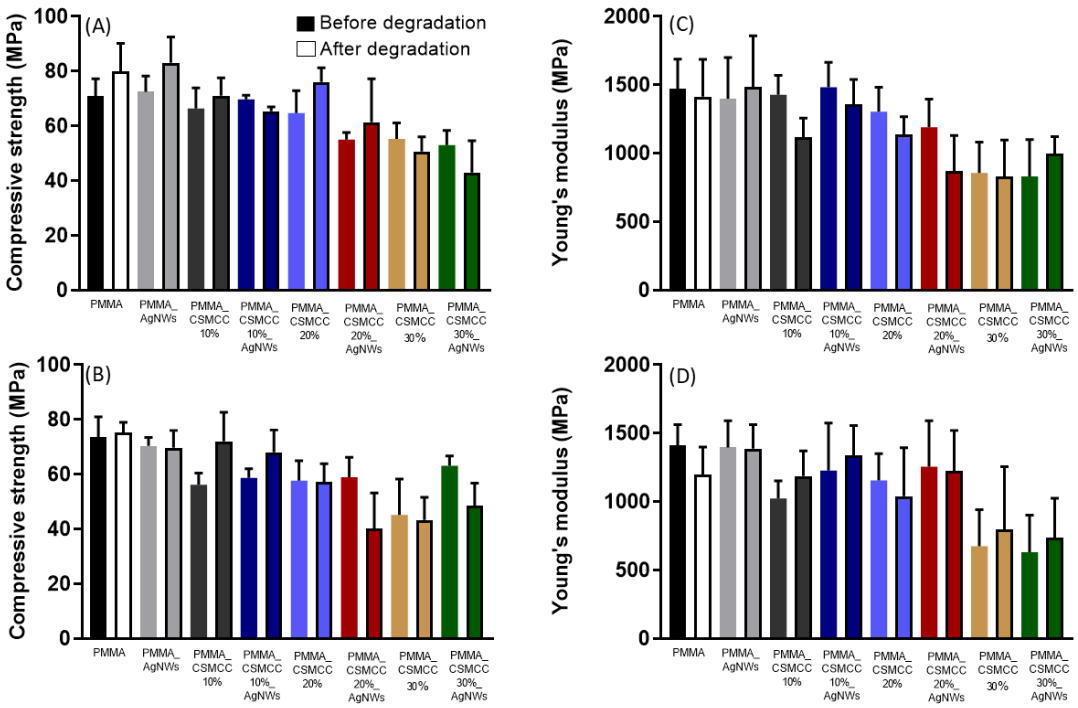

Figure S4. Compressive strength (**A** and **B**) and Young's modulus (**C** and **D**) of PMMA-based cements containing CSMCC, before (no border) and after compression (black border). (A and C) cements with P/L 2:1 and (B and D) cements with P/L 2:0.8.

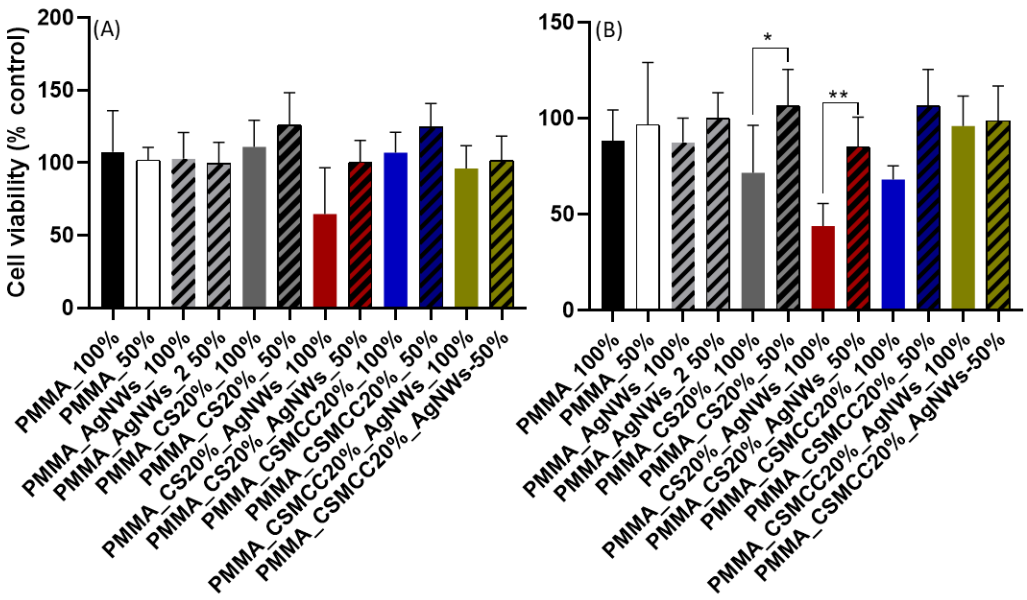

Figure S5. Cytotoxicity of cement eluates at different dilutions (100% vs 50%) on mesenchymal stem cells after **(A)** 1 and **(B)** 2 days of incubation. Cytotoxicity was tested against the cements eluates. P/L ratio 2:1. Data are reported as mean ± SD (n≥3). Results of the t-test are reported in the graph: *p< 0.05 and **p< 0.01.

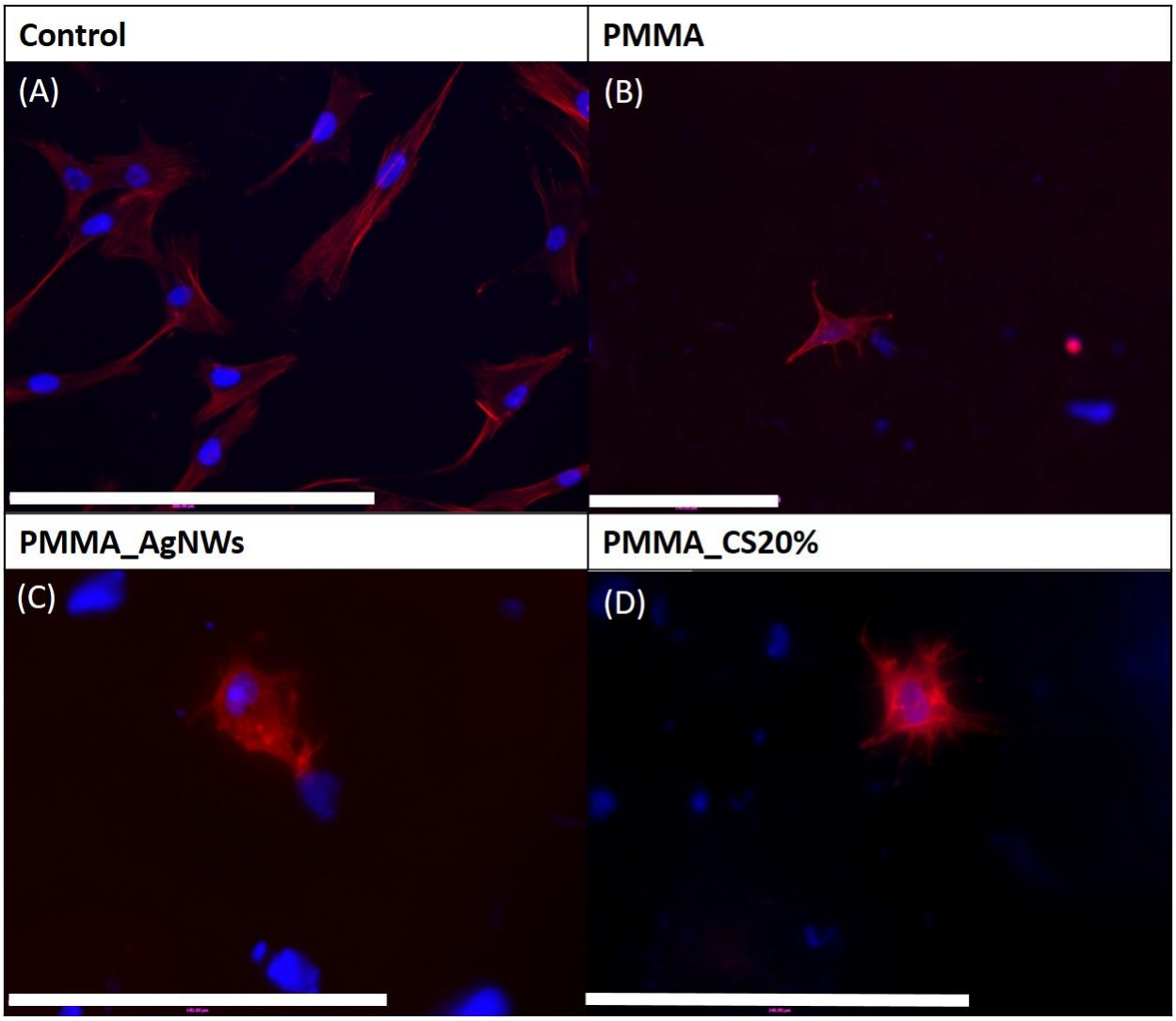

Figure S6. Morphology of MSCs cultured on **(A)** glass slide, **(B)** PMMA cement, **(C)** PMMA_AgNWs cement and **(D)** PMMA_CS20% cement, at 24 hours. DAPI was used to counterstained nuclei and Phalloidin Dylight 550 was used to counterstained actin. Scale bars: (A) 200 µm, (B) 140 µm, (C) 140 µm and (D) 140 µm.

Morphological analysis (Fig. S6) showed that MSCs were well spread and distributed on the control (glass slide), with a characteristic fusiform-like shape. On the other hand, the cells on cements displayed a less elongated shape and they were less in number, suggesting a lower cytocompatibility than the control.

References

(1) Zhao, Y.-N.; Fan, J.-J.; Li, Z.-Q.; Liu, Y.-W.; Wu, Y.-P.; Liu, J. Effects of Pore Size on the Osteoconductivity and Mechanical Properties of Calcium Phosphate Cement in a Rabbit Model. *Artif. Organs* **2017**, *41* (2), 199–204. https://doi.org/10.1111/aor.12742.

(2) de Wild, M.; Zimmermann, S.; Rüegg, J.; Schumacher, R.; Fleischmann, T.; Ghayor, C.; Weber, F. E. Influence of Microarchitecture on Osteoconduction and Mechanics of Porous Titanium Scaffolds Generated by Selective Laser Melting. *3D Print. Addit. Manuf.* **2016**, *3* (3), 142–151. https://doi.org/10.1089/3dp.2016.0004.